Mapping 3D breast lesions from full-field digital mammograms using subject-specific finite element models.

E. García[a], A. Oliver[a], O. Diaz[a], Y. Diez[b], A. Gubern-Mérida[c], R. Martí[a], and J. Martí[a]

[a]Institute of Computer Vision and Robotics, University of Girona, Spain
[b]Tokuyama Laboratory GSIS, Tohoku University, Japan
[c]Radboud University Medical Center, Nijmegen, The Netherlands

ABSTRACT

Patient-specific finite element (FE) models of the breast have received increasing attention due to the potential capability of fusing images from different modalities. During the Magnetic Resonance Imaging (MRI) to X-ray mammography registration procedure, the FE model is compressed mimicking the mammographic acquisition. Subsequently, suspicious lesions in the MRI volume can be projected into the 2D mammographic space. However, most registration algorithms do not provide the reverse information, avoiding to obtain the 3D geometrical information from the lesions localized in the mammograms. In this work we introduce a fast method to localize the 3D position of the lesion within the MRI, using both cranio-caudal (CC) and medio-lateral oblique (MLO) mammographic projections, indexing the tetrahedral elements of the biomechanical model by means of an uniform grid. For each marked lesion in the Full-Field Digital Mammogram (FFDM), the X-ray path from source to the marker is calculated. Barycentric coordinates are computed in the tetrahedrons traversed by the ray. The list of elements and coordinates allows to localize two curves within the MRI and the closest point between both curves is taken as the 3D position of the lesion. The registration errors obtained in the mammographic space are 9.89 ± 3.72 mm in CC- and 8.04 ± 4.68 mm in MLO-projection and the error in the 3D MRI space is equal to 10.29 ± 3.99 mm. Regarding the uniform grid, it is computed spending between 0.1 and 0.7 seconds. The average time spent to compute the 3D location of a lesion is about 8 ms.

Keywords: Breast MRI, Full-Field digital Mammography, Multi-modal registration, Finite Element modelling

1. INTRODUCTION

Magnetic resonance imaging (MRI) and X-ray mammography are two image modalities used to diagnose breast diseases in women. X-ray mammograms are considered the gold-standard in early breast disease detection. However, the 2D-projection makes locating suspicious lesions within the uncompressed breast difficult. In contrast, MRI provides this information at the cost of having less image resolution. Therefore, both modalities provide complementary information and, hence, the combination of these modalities is crucial to increase both the early diagnosis and biopsy procedures. During past decades, the efforts have been focused on establishing spatial correlation between both modalities. Subject-specific 3D finite element (FE) modeling of the breast has received increasing attention. To correlate MRI and mammographic images, the overall process consists in mimicking the mammographic acquisition, compressing the FE model and simulating the X-ray beam. The model is allowed to translate and rotate, while the elastic parameters can be modified in order to reach an accurate correspondence.

Most of the registration methods are limited to providing the distance of projected lesions from MRI with respect to the lesion within the mammogram. But they do not provide 3D geometrical information of the suspicious lesion within the MRI when they are located in the mammograms. Some exceptions can be found in the literature that consist in complex or computationally expensive approaches. Qiu et al.[1,2] use a 3D FE model to register temporal mammograms. The process consists in compressing the mechanical model and aligning it with the correspondent mammographic view (cranio-caudal (CC) or medio-lateral oblique (MLO)). A back-projection ray-cast is applied and the elements traversed by the X-ray's path are labeled. The compressed model is restored to the reference state and the straight line becomes a 3D curve in the initial model. When both CC and MLO projections are available, the 3D lesion is localized finding the minimum distance between both 3D curves. Hopp et al.[3] describe a similar approach to localize lesions within MR images using a patient-specific

Medical Imaging 2017: Image-Guided Procedures, Robotic Interventions, and Modeling, edited by Robert J. Webster III, Baowei Fei, Proc. of SPIE Vol. 10135, 1013504 · © 2017 SPIE
CCC code: 1605-7422/17/$18 · doi: 10.1117/12.2255957

model. Mertzanidou et al.[4] use a complex transformation to correlate the uncompressed and the compressed model. This transformation is performed during the ray-casting step and consists in undoing the transformation considering the rigid (translation and rotation) and non-rigid transformation (interpolating displacements within the FE model) to which the model is subjected. Solves-Llorens et al.[5] use the tetrahedrons which compose the model to localize lesions before and after compression, as well as between the MRI and mammograms. This method avoids decompressing the model and carrying out complex transformations. However, it may result slow depending on the number of elements composing the FE model.

Data structures are used in computer graphics to accelerate ray-casting and visualization. These structures use surface meshes composed of triangular elements, although some of them can be adapted to any other kind of elements, such as tetrahedral elements. In this work we use one of these structures to accelerate the localization of the ray from the compressed model to the MRI volume. Specifically, we use an uniform grid, adapting the work introduced by Lagae et al.,[6] to index the elements of the biomechanical model. Hence, the position of the sampled points along the ray can be simultaneously localized in the compressed model and the MRI, by means of computing the barycentric coordinates within the elements traversed by the ray. When both CC- and MLO-curves have been localized in the MRI, the search space of the intersection is reduced using a set of rules, and we obtained an accurate and fast navigation between both image modalities.

The rest of this document is organized as follows: Section 2 introduces the methodology used. We present the registration approach, the uniform grid construction and, finally, the fast 2D-3D correspondence method. Section 3 presents the results regarding the registration and the grid construction. We conclude the paper with discussion and conclusions.

2. MATERIAL AND METHODS

The dataset was composed of 10 cases from 10 different patients. Each case contains 1 MRI volume and 1 mammographic study, using full-field digital mammograms (FFDM), composed of both CC and MLO projections. Patients aged between 37 and 63 (48.8 ± 9.59). Images were acquired at the Radboud University Medical Center (Nijmegen, The Netherlands) between July 2008, and May 2011. The MRI scanner used was a 1.5 Tesla Siemens scanner (Magnetom Vision, Magnetom Avanto and Magnetom Trio) with dedicated breast coil (CP Breast Array, Siemens, Erlangen). MRI volumes had a size of $[512 \times 256 \times 120]$ voxels and $[0.664 \times 0.664 \times 1.300]$ mm^3 per voxel. Regarding the mammographic device, the images were acquired by either a GE Senographe 2000D or GE Senographe DS, according to the standard clinical settings. Mammograms were composed of $[2294 \times 1914]$ pixels, with $[0.094 \times 0.094]$ mm^2 per pixel. Both MRI and mammographic studies were acquired in the same day. The lesions were labeled by an expert medical image researcher.

This work was performed on a workstation Intel Core i7-3770 3.40 GHz, RAM 32 Gb, 64 bits equipped with a GPU NVIDIA GeForce GTX 770 (2 Gb).

2.1 MRI-FFDM registration

To obtain the FE model, MRI volumes are segmented by means of a probabilistic atlas approach, using a methodology similar to the one proposed by Gubern-Mérida et al.[7] The internal tissues of the breast are segmented using an expectation-maximization algorithm, while the breast mask images are resampled to obtain isotropic voxels. Afterwards, two different meshes are constructed by means of the standard Marching Cubes algorithm,[8] corresponding to the breast surface and glandular tissue. We use the open-source package TetGen[9] to build tetrahedral meshes, with the number of elements determined using a maximum volume criterion which is related to the MRI voxel volume. The stress-strain relationship of the biomechanical model is approximated by a nearly incompressible, isotropic and hyperelastic neo-Hookean model for each tissue (glandular and adipose), using the corresponding Young's modulus measured by Wellman.[10]The breast-body interface is fitted to a linear surface and nodes belonging to this surface are allowed to slide in the parallel direction of the compression paddle displacement.[11]

Once the biomechanical model has been built, it is duplicated in order to get both the uncompressed and the compressed models. For obtaining the latter, the necessary information to reproduce the acquisition (breast thickness, projection angle, source-to-detector distance or maximum tube voltage) is extracted from the DICOM

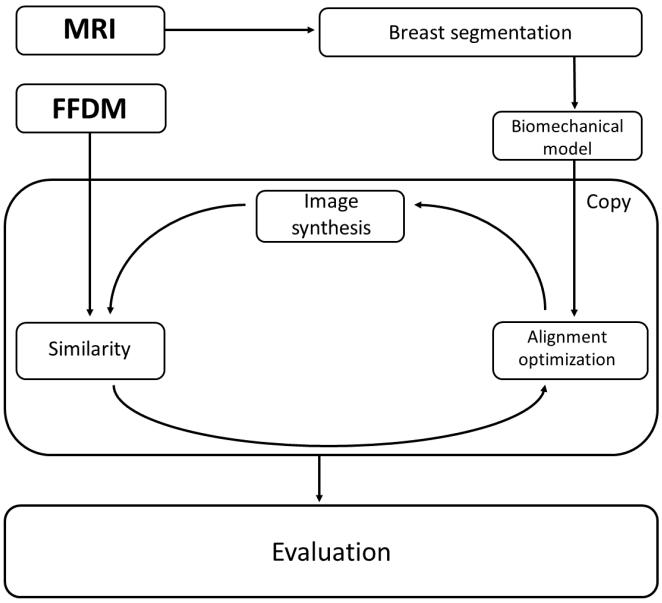

Figure 1. The registration approach. Beginning from the MRI, the breast is segmented and the biomomechanical model is built. This model is used to correlate the information of the MRI volume and FFDM mammograms. The final step is to evaluate the accuracy of this correlation.

header of the corresponding FFDM. The ray-casting is accelerated by a GPU implementation. The simulated annealing algorithm[12] is used to optimize the location and material parameters of the model.[4] The optimization process consists in finding the maximum Normalized Cross-Correlation between the actual and synthetic mammogram. Therefore, the parameters to optimize are:

- Position: translation of the model along a plane parallel to the mammogram.
- Orientation: the model is allowed to rotate around its principal axes.
- Elastic parameters: in this case, the Young's modulus of both adipose and glandular tissues.
- Compression: the breast thickness.

Eventually, uncompressed and compressed models of the breast are available. The former relates the physical space of the MRI volume while the compressed model is localized above the space defined by the mammogram. Figure 1 summarizes the registration process.

During this work, the FE analysis was performed using NiftySim^{TM} v.2.3.1[13] (University College London*). NiftySim^{TM} solves the Total Lagrangian Explicit Dynamic (TLED) FE formulation proposed by Miller et al.[14] for soft-tissue simulations.

2.2 Fast correspondence

Usually, to evaluate the accuracy of the algorithm, a target registration error (TRE) approach is performed using the lesions presented in both modalities. The 2D TRE is computed as the Euclidean distance between the centroid of the lesion localized in the MRI, projected in the mammography, and the centroid of the lesion in the mammogram. Figure 2 shows an example of both the real lesion in a mammogram and the projected one from the MRI volume.

Nevertheless, as we expose in section 1, the 3D TRE requires of complex approaches that, usually, include the decompression of the breast model. In our approach, we build a data structure to index the elements of the

*https://sourceforge.net/projects/niftysim/

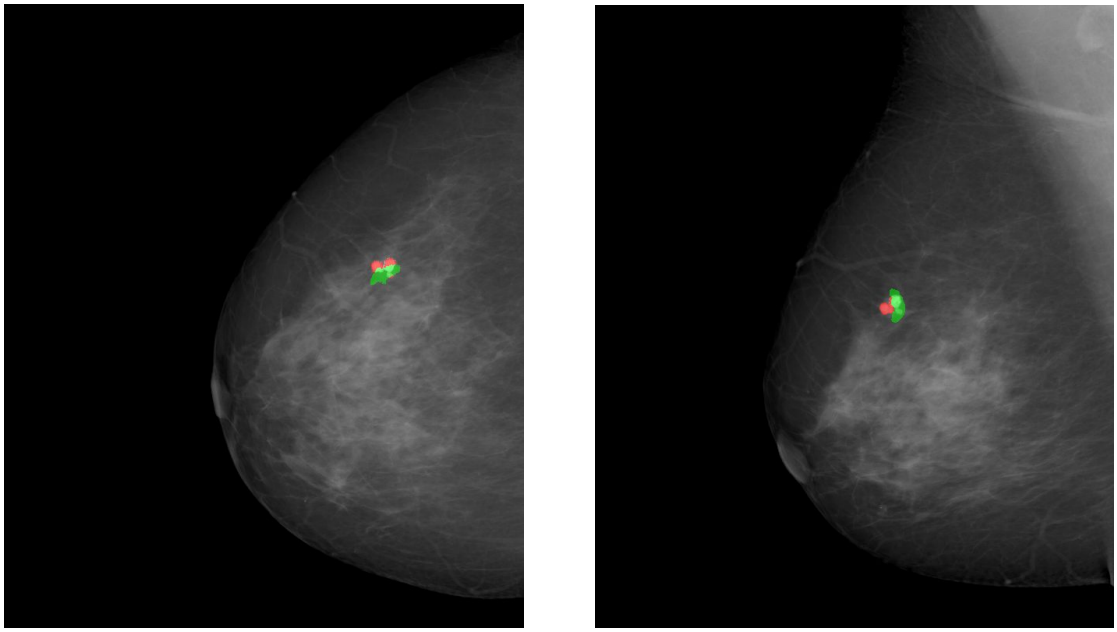

Figure 2. CC and MLO mammograms of the same patient. The red area corresponds to the suspicious regions in the mammograms, while the green area represents the location of the MRI lesion, once the registration has been performed.

model. The ray traversing the compressed model is localized automatically in the uncompressed model, at the same time. Using both, the ray traversing the CC- and that traversing the MLO- model, in the MRI volume, the intersection is computed by using a set of rules to reduce the search space among the points. The following sections explain the construction of the grid and the search space reduction.

2.2.1 Uniform grid construction algorithm

When the biomechanical breast model reaches the optimal position with respect to the mammogram, an uniform grid is used to store the element indexes of the compressed breast. The overall process to build this grid consists in:

- First, the bounding box of the compressed breast model is computed. The origin, size and spacing of the grid are established to initialize the grid around the model.
- The Axis-Aligned Bounding Boxes (AABB) of all elements in the compressed breast model are calculated.
- The uniform grid obtained is composed of three arrays:
  - The first array corresponds to the number of events, number of AABB, overlapping each voxel in the grid.
  - The second array computes the accumulative sum of all previous events of the first array.
  - The third array corresponds to the element list. This array is initialized with length equal to the total sum of events indexed in the first array. The corresponding element number is allocated using the sum of events before the voxel plus the corresponding position of the event in the voxel.

The time complexity of this algorithm is linear in the number of elements.

2.2.2 2D-3D correspondence

To provide the location of the breast lesion within the MRI volume from FFDM, the lesion has to be visible and specified in both CC and MLO projections. Once the lesion is localized in the mammograms, the projection from the X-ray source to the lesion is defined. The ray is described by the parametric equation of the straight line. Sampling the ray is carried out incrementing the parametric value.

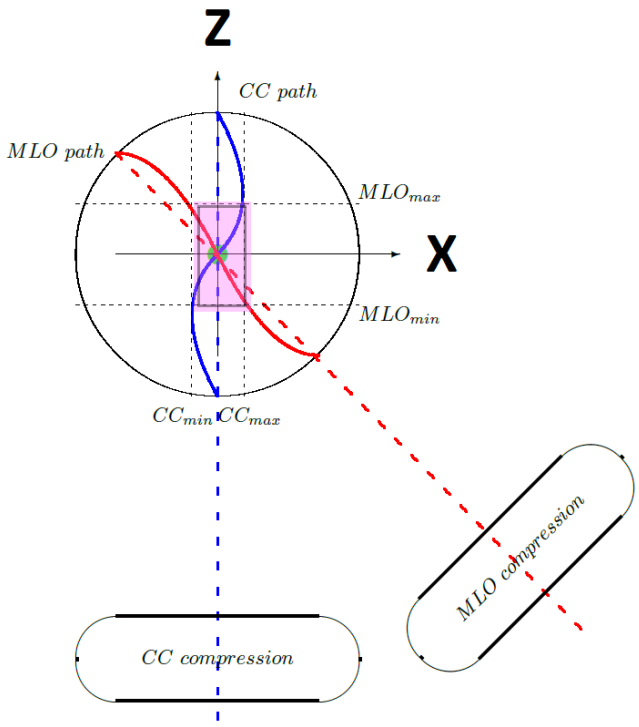

Figure 3. Both CC- and MLO- paths are represented by the blue and red curves, respectively, from their respective compressed models. The purple region represents the reduced search space where the 3D lesion (green dot) is localized.

To localize a given path within the MRI volume, for each sampled point along the ray's path, the corresponding voxel in the grid is computed from its physical position. For each element belonging to the voxel, the barycentric coordinates are computed. If the point is inside the element, the barycentric coordinates are used to localize the position in the uncompressed model. Thus, all points belonging to one ray in the compressed model are moved to the uncompressed model, obtaining a curve in the MR image.

Using both CC- and MLO- curves, we localize the suspicious lesion within the image using the minimum distance between both curves. However, we also speed-up the procedure by reducing the search space as follows:

- First, both curves are projected in the anterior-posterior (Y) direction.
- The minimum (CC_{min}) and maximum (CC_{max}) of the CC-ray in the medial-lateral (X) direction are computed in order to reduce the search space.
- Points belonging to the MLO-ray outside of the interval $[CC_{min},\ CC_{max}]$ are not considered.
- The maximum (MLO_{max}) and minimum (MLO_{min}) in the inferior-superior (Z) direction are computed, using the valid points of the MLO-ray. The points belonging to the CC-ray outside of the interval are excluded.

Thus, the search space is reduced between $[CC_{min},\ CC_{max}]$ in the X direction and $[MLO_{min},\ MLO_{max}]$ in the Z direction. The Euclidean distances between the points belonging to the CC-ray and the MLO-ray within both intervals are computed, and the center of mass of the two points with the smallest distance is considered the 3D center of the lesion. Figure 3 represents the anterior-posterior projection of the breast, traversed by the CC- (blue) and the MLO- (red) rays.

Table 1. Number of points and elements composing each model, as well as mean number of elements per voxel in the grid, $mean_{CC}$ and $mean_{MLO}$, and time of construction, t_{CC} and t_{MLO}, in seconds, for both CC- and MLO-projections.

	#points	#elements	$mean_{CC}$	t_{CC}	$mean_{MLO}$	t_{MLO}
Case 1.	10,458	61,559	13.91	0.354	11.12	0.252
Case 2.	8,811	49,895	11.92	0.156	10.43	0.087
Case 3.	14,701	78,098	11.83	0.215	13.22	0.340
Case 4.	13,467	79,796	14.36	0.256	10.52	0.190
Case 5.	17,979	98,574	12.67	0.303	10.52	0.373
Case 6.	43,556	260,444	17.24	0.613	16.11	0.647
Case 7.	9,056	52,242	12.86	0.108	11.55	0.066
Case 8.	10,977	57,555	14.96	0.213	12.82	0.271
Case 9.	5,908	32,245	14.18	0.068	11.46	0.078
Case 10.	7,525	41,880	13.24	0.420	12.00	0.169

Table 2. Number of points composing each ray and final number of points to be checked after the search space reduction. Furthermore, we include the minimum separation between both rays, in millimeters, and time of computing the intersection, in seconds.

	Ray_{CC}	Ray_{MLO}	Separation (mm)	Time (s)
Case 1.	13/ 798	19/ 753	8.16	0.008
Case 2.	37/ 609	68/ 786	2.93	0.014
Case 3.	15/ 738	21/ 810	9.06	0.011
Case 4.	16/ 741	28/ 936	0.75	0.005
Case 5.	45/ 942	84/1302	6.93	0.016
Case 6.	23/1023	40/ 957	0.35	0.005
Case 7.	13/ 477	29/ 444	0.91	0.004
Case 8.	57/ 678	82/ 714	1.85	0.006
Case 9.	2/ 468	6/ 606	0.56	0.004
Case 10.	17/ 768	29/ 708	2.70	0.005
mean	23.8/ 727.2	40.6/ 801.6	3.42 ± 3.35	0.008 ± 0.005

3. EXPERIMENTAL RESULTS

Biomechanical models are built from precontrast T1-weighted MRI. The number of elements composing the breast model depends on the MRI voxel volume and the total volume of the breast and, therefore, is different for each model. In our data set, the number of points composing each model range between 5,908 and 43,556, while the number of elements vary from 32,245 to 260,444. Once the registration is performed, the uniform grid is built around the compressed breast model to store the element indexes. The accuracy of the grid depends on internal factors, such as the grid resolution or the voxel size, and external factors, such as the number of elements composing the model as well as the amount of compression. Based on previous experiments, we use a 2-mm length voxel to define the grid. Origin and size are determined by the axis-oriented bounding box of the compressed model. Table 1 shows the statistical analysis of our dataset, points and elements composing each model, mean number of elements per voxel in the grid and the time of grid construction, in seconds.

We use the backprojection from the centroid of the lesion localized within the mammogram to simulate each ray traversing the corresponding compressed model, but we only consider those points that are inside of the model. Hence, the length of each ray depends on the thickness of the biomechanical model, once it was compressed. During this study, the maximum number of points along a ray was 1,302 points, while the minimum was 444. As is usual, checking the distance point-by-point, the number of combinations varies between 200,000 (case 7) and 1,250,000 (case 5) in our data set. Using our approach for search space reduction, the number of points to be checked is drastically reduced. The best result is obtained in the case 9, where the number of combinations in the final search space is 12 (6×2 points) from 283,608 (468×606 points) possible combinations at the beginning. The mean value for the search space reduction is 1,378 from 611,783 combinations in our dataset. Therefore, the search space is reduced 1/600 approximately. Table 2 shows more detailed information about the space reduction, considering each projection independently.

Table 3. Detailed information of the target registration error, in millimeters, in 2D and 3D.

	c1	c2	c3	c4	c5	c6	c7	c8	c9	c10	mean	std
CC	7.50	11.37	17.11	5.14	11.52	6.03	8.20	7.10	12.31	7.05	9.89	3.72
MLO	17.65	8.63	14.16	7.21	4.31	4.48	4.04	5.66	9.98	4.25	8.04	4.68
MRI	11.06	15.93	13.64	7.51	9.671	3.30	8.35	10.11	7.50	7.45	10.29	3.99

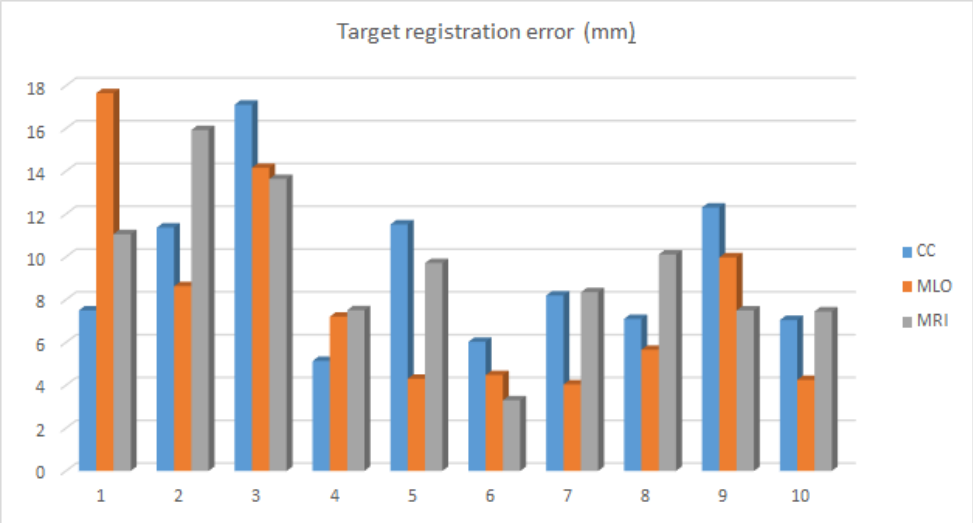

Figure 4. Target registration errors, in millimeters, obtained using our registration algorithm.

Finally, the MRI-mammography registration spends between 2 and 5 hours and the error evaluation is performed as exposed in section 2.2.2. The final TRE results are presented numerically in table 3 and graphically in figure 4. The best result in 2D is about 5 mm and 3 mm in 3D. Mean error values correspond to $9.89 \pm 3.72\, mm$ in CC-, $8.04 \pm 4.68\ mm$ in MLO-projection and $10.29 \pm 3.99\ mm$ in the MRI volume.

4. DISCUSSION AND CONCLUSIONS

In this work we introduced a fast approach to localize lesions between MRI and X-ray mammograms using a finite element model combined with a uniform grid to correlate both modalities. This method allows to localize small lesions like microcalcifications and masses in the 3D MRI when they are located in both CC and MLO mammographic views. Regarding the data structure, the uniform grid provides an accurate method to index the elements. Its main advantage compared to other data structures, such as octrees or kd-trees, is that it is easier to implement and faster to build than the others. Furthermore, due to the breast is compressed between parallel paddles, the grid is almost fulfilled and tracing the ray through the grid requests less computational requirements. The errors reported in our study are 9.89 mm in CC and 8.04 mm in MLO, in line with those reported by Mertzanidou et al.,[4] and 10.29 mm in the 3D volume, smaller than Hopp et al.[3] . The time spent to compute the 3D location of the lesion, once the mammograms and the MRI are registered, is about 8 ms, allowing its use in real time applications.

Once the registration is performed, several clinical applications can be developed. For instances, we can use the biomechanical model to obtain the registration between CC and MLO views (ipsilateral registration), which can be very useful for correlation the different breast structures. Moreover, this step can help int he computation of multimodal features for CAD algorithms of the fast tracking of the needle biopsy between modalities. Furthermore, assuming that there is not a significant change of the breast tissues between two time points, we could use he same biomechanical model to correlate temporal mammogram, helping the radiologist to evaluate the temporal evolution of susceptible areas.

5. ACKNOWLEDGEMENT

This research has been partially supported from the University of Girona (MPC UdG 2016/022 grant), the European Union within the Marie Sklodowska-Curie Innovative Training Networks (SCARtool project H2020-MSCA-IF-2014, reference 657875) and the Ministry of Economy, Industry and Competitiveness of Spain, under project SMARTER (DPI2015-68442-R) and the FPI grant BES-2013-065314.

REFERENCES

[1] Qiu, Y., Sun, X., Manohar, V., and Goldgof, D., "Towards registration of temporal mammograms by Finite Element simulation of MR Breast volumes," *Proc. SPIE Med. Imag.* **1**, 69182F–69182F, International Society for Optics and Photonics (2008).

[2] Qiu, Y., Goldgof, D., Li, L., Sarkar, S., Zhang, Y., and Anton, S., "Correspondence recovery in 2-view mammography," *IEEE Biomed. Imag.: Nano to Macro* **1**, 197–200, IEEE (2004).

[3] Hopp, T. and Ruitter, N., "2D/3D registration for localization of mammographycally depicted lesions in breast MRI," *IWDM 2012* **7361**, 627–634 (2012).

[4] Mertzanidou, T., Hipwell, J., Johnsen, S., Han, L., Eiben, B., Taylor, Z., Ourselin, S., Huisman, H., Mann, R., Bick, U., et al., "MRI to X-ray Mammography intensity-based registration with simultaneous optimisation of pose and biomechanical transformation parameters," *Med. Imag. Analysis* **18**(4), 674–683 (2014).

[5] Solves-Llorens, J. A., Rupérez, M., Monserrat, C., Feliu, E., García, M., and Lloret, M., "A complete software application for automatic registration of X-ray mammography and magnetic resonance images," *Med. Phys.* **41**(8), 081903 (2014).

[6] Lagae, A. and Dutré, P., "Compact, fast and robust grids for ray tracing," *Comp. Graphics* **27**(4), 1235–1244, Wiley Online Library (2008).

[7] Gubern-Mérida, A., Kallenberg, M., Platel, B., Mann, R., Martí, R., and Karssemeijer, N., "Volumetric breast density estimation from full-field digital mammograms: A validation study," *PLoS One* **9**(1), e85952 (2014).

[8] Lorensen, W. and Cline, H., "Marching Cubes: A high resolution 3D surfaces construction algorithm," *ACM Comp. Graphics* **21**(4), 163–169 (1987).

[9] Si, H., "TetGen. A Delaunay-based quality tetrahedral mesh generator," *ACM Trans. Math. Software* **41**(2), 1–36 (2015).

[10] Wellman, P., *Tactile imaging*, PhD thesis, Cambridge, MA: Harvard University's Division of Engineering and Applied Sciences (1999).

[11] Han, L., Hipwell, J., Tanner, C., Taylor, Z., Mertzanidou, T., Cardoso, J., Ourselin, S., and Hawkes, D., "Development of patient-specific biomechanical models for predicting large breast deformation," *Phys. Med. and Bio.* **57**(2), 455–472 (2012).

[12] Kirkpatrick, S., Gelatt, C. J., and Vecchi, M., "Optimization by simulated annealing," *Science* **220**(4598), 671–680 (1983).

[13] Johnsen, S., Taylor, Z. A., Clarkson, M., Hipwell, J., Modat, M., Eiben, B., Han, L., Hu, Y., Mertzanidou, T., Hawkes, D. J., and Ourselin, S., "NiftySim: A GPU-based nonlinear finite element package for simulation of soft tissue biomechanics," *J. Comp. Assisted Radiology and Surgery* **10**(7), 1077–95 (2014).

[14] Miller, K., Joldes, G., Lance, D., and Wittek, A., "Total lagrangian explicit dynamics finite element algorithm for computing soft tissue deformation," *Comm. Num. Meth. Eng.* **23**(2), 121–134 (2007).